

Multi-scale characterization of carbon-fibre reinforced PEEK composites manufactured by laser-assisted tape placement

RESTIF Noé^{1,2,a*}, LAIK Suzanne¹, PERON Mael²,
DAGHIA Federica³, JACQUEMIN Frederic²

¹CETIM, Technocampus Composites, Chemin du Chaffault, 44340 Bouguenais, France

²Nantes Université, Ecole Centrale de Nantes, CNRS, GeM, UMR CNRS 6183, 44600 Saint-Nazaire, France

³Université Paris-Saclay, CentraleSupélec, ENS Paris-Saclay, CNRS, LMPS - Laboratoire de Mécanique Paris-Saclay, 91190, Gif-sur-Yvette, France

^anoe.restif@cetim.fr

Keywords: Thermoplastic Composites, PEEK, Tape Placement, Experimental Characterization

Abstract. The Laser-Assisted Tape Placement forming process of thermoplastic composites enables the rapid production of laminates. However, it requires the tuning of the processing parameters, which is currently limited by a misunderstanding of the consolidation phenomena occurring during process and the interlaminar properties related with strong welded interfaces. This study aims at establishing correlations between physical properties and mechanical strength of welded thermoplastic composites, by using several methods and characterizations at different scales. Carbon-fibre reinforced PEEK (CF/PEEK) composites produced by a LAMP process were investigated by varying the Laser Setpoint Temperature (LST) and Tool Temperature (TT). The results show that laminates manufactured at a LST of 350 °C have high void content, with the location of the voids depending on the TT: at a TT of 25 °C (unheated tool), interply and intraply voids are present while for a TT of 250 °C they are mainly intraply. Laminates produced at a LST of 450 °C also have mainly intraply voids, although their void content is significantly lower than that of laminates produced at an LST of 350 °C. For laminates having mainly intraply voids, ILSS testing demonstrates failure by an intralaminar failure mode. An increase in intralaminar shear strength is observed as the intraply void content decreases and the degree of crystallinity increases, related to the LST and the TT. The combination of experimental techniques thus allowed to provide understanding on the influence of local physical properties of the composites manufactured by LAMP on specific interface-related mechanical properties, and demonstrate that, despite variations of mechanical performances with processing conditions, interfaces are no longer a weak point within the laminates when the processing conditions allow for sufficient intimate contact to occur during the consolidation phase.

Introduction

Thermoplastic matrix composites are increasingly used in the aeronautic and automotive industries due to their many advantages over thermoset matrix composites. These advantages include their better impact resistance and toughness and their potential for being reused or even recycled. Also, the forming of laminates by « out of autoclave » fusion bonding processes is more environmentally sustainable. The LAMP was identified as an efficient and versatile process to manufacture high performance and complex-shaped parts. However, this process involves several complex and interdependent consolidation and deconsolidation phenomena within very short times [1]. At first, increasing the temperature and then the pressure allows the establishment of intimate contact [2]. Then, healing of the material takes place [2], [3]. It corresponds to the inter-diffusion

of molecular chains from one surface to another [4] and it strongly depends on time and temperature [2], [3], [5]. During cooling, crystallization can occur and is promoted by a low cooling rate. Moreover, deconsolidation mechanisms of the incoming tape and the previously consolidated laminate (substrate) can occur during layup. The deconsolidation mechanisms which affect the void content are the void growth into rich resin area and confined fibers area [6], [7], [8]. Recent work on hot pressed laminates [8] showed that a significant growth of voids requires melting of the matrix, while a preliminary phase of voids nucleation can take place above the glass-transition temperature (T_g).

Current knowledge is not sufficient to establish the interaction between these phenomena, and their effect on laminate mechanical properties. Many authors are establishing the link between the processing parameters and the laminate mechanical properties, showing an increase in shear strength with an increase of the TT or the LST [9]. However, there are only a few studies relating an increase in shear strength to the consolidation phenomena, by characterizing physical properties at the welded interface [10], [11]. Most studies investigating physicochemical characterization have correlated the increase in shear strength as a result of the change in the processing parameters with a void content decrease [12], [13], [14]; however, only a few investigations on the failure mode were described, and when it was described it is often interlaminar, even for autoclaved manufactured laminates [14]. It means that even for optimal manufacturing conditions, the interply remains the weakest area of the laminate, which raises many questions about the material and process quality. However, Comer et al. [15] show the major presence of intraply voids within ATP laminates, together with a decrease of the ILSS performance, though they did not relate the failure mode to the presence of these intraply voids.

This study aims at establishing links among the processing parameters, the physical properties associated with the consolidation phenomena and the shear strength and corresponding failure mode of PEEK/CF laminates. The experimental method consists of two steps: (i) investigate the influence of the manufacturing conditions over the mechanical properties by ILSS testing with a critical investigation of the failure mode (interply or intraply); and (ii) characterize the relationship between physical properties and the aforementioned mechanical properties.

Materials and Method

Materials. Laminates were produced using unidirectional carbon fibre reinforced PEEK tape of 0.23-mm thick and 18-mm wide. PEEK's glass transition temperature (T_g) and melting temperature (T_m) were measured by Differential Scanning Calorimetry (DSC) on the as-received material leading to 143.3 °C and 344.6 °C, respectively, for a degree of crystallinity of 25.2 ± 0.2 %. The void content was measured on micrographs of embedded and micron-polished tape section and was concluded to be 0.49 ± 0.4 %. Due to confidentiality matters, further information about the material cannot be disclosed.

Process. The production of laminates (containing two flat sides) was performed at CETIM using SPIDE TP®. It is a LAMP and filament winding process (Fig. 1). During processing, the LAMP head (from AFPT GmbH) winds the tape around the oblong tool in the y direction shifting of one tape width along its course on one flat side over each lap, allowing for continuous deposition of the layers. Meanwhile, the tool is rotated in the opposite direction to the layup direction of the tape. For all manufactured parts, a number of 30 layers was laid up, resulting in approximately 6-mm thick laminates. The two processing parameters that were varied in this study were the LST (350 and 450 °C), and the TT (25 and 250 °C). The laser power and tilt were continuously regulated through a feedback temperature loop set on the LST and based on the measurement of the illuminated tape and substrate area by an embedded infrared camera. All processing parameters are given in Table 1, including the average laser power for each LST and corresponding average standard deviation between the plies. Because of limited space, more detailed data (e.g. variation of power within plies or evolution between the first and the last ply) are not provided in this paper.

Laminates are identified through both parameters with the following reference code type “TT/LST”. For all laminates, the layup speed was set to 5 m/min and a consolidation force of 250 N was applied by a 60-shore silicon compaction roller.

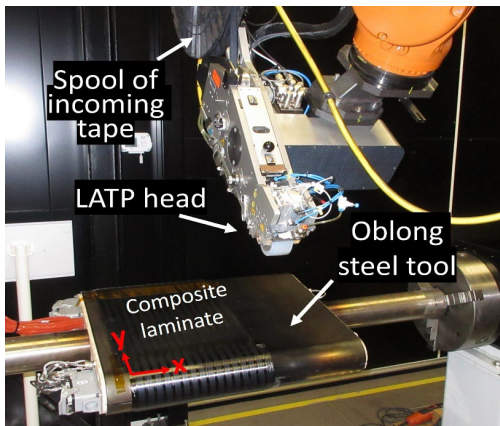


Table 1 – Manufacturing conditions of laminates with all processing parameters programmed by SPIDE TP®

Reference	Tool Temperature (TT) [°C]	Laser Setpoint Temperature (LST) [°C]; Laser average power [W]
25/350	25	350; 924 ± 32
250/350	250	350; 653 ± 53
25/450	25	450; 1271 ± 65
250/450	250	450; 1012 ± 43

Figure 1 – SPIDE TP® Process

Optical Microscopy (OM). All images of laminate cross-sections were produced with an optical microscope ZEISS AXIOSCOPE 5. The samples were prepared by being embedded in a resin and polished using sandpapers from P500 down to 1 μm grit size. An area of approximately 10-mm wide over the entire thickness of each laminate was analysed. The void content was calculated in both intralaminar and interlaminar regions using ImageJ software.

Ultrasonic (US) testing. All the laminates were controlled by US nondestructive testing through C-Scan and A-Scan to check for local defect indications and/or obtain relative attenuation levels. In the absence of local defects, global attenuation as compared to a healthy laminate of the same material could be attributed to diffuse porosity. Results are given in %SH (screen height) which is a relative unit based on a signal gain set on a reference material of the same nature with known good material health level.

Scanning Electronic Microscopy (SEM). A ZEISS SUPRA 25 scanning Electron Microscope was used at an acceleration voltage of 15 kV to analyze the fracture surfaces of mechanically tested specimens. Specimens were metallized with Platinum prior to observation.

Differential scanning calorimetry (DSC). DSC analyses were performed using a Mettler TOLEDO DSC 3. To obtain results over the entire thickness of the laminates, sampling consisted of cutting a thin cross-section using a microtome. Samples of approximately 10 mg were placed in 40 μl aluminum pans, with non-hermetically sealed lids. Two temperature ramp-ups and -downs were performed at heating rates of 10 °C/min between room temperature and 380 °C. Three sample were analysed for each laminate in a nitrogen environment (to avoid any sample oxidation) at a flow rate of 50 ml/min. The degree of crystallinity of a sample was estimated by using Eq.1:

$$X = \frac{\Delta H_m - \Delta H_{cc}}{(1 - \omega) \times \Delta H_{m\infty}} \quad (1)$$

where ΔH_m is the melting enthalpy, ΔH_{cc} is the cold crystallization enthalpy, ω is the weight fraction of matrix content, and $\Delta H_{m\infty}$ is the theoretical melting enthalpy of 100% crystalline PEEK which has been calculated to be 130 J/g by Blundell et al. [16].

Interlaminar shear strength (ILSS) testing. The interlaminar shear behavior of laminates was assessed by following the ASTM D2344 Standard, using a span-to-thickness ratio of 4:1. Five specimens measuring 40 x 12 x t mm (t is the thickness, being approximately 6 mm) were tested

for each laminate. Testing was performed at 1 mm/min on an INSTRON 3369 tensile testing machine with a maximum load capacity of 10 kN. The apparent interlaminar shear strength is calculated using Eq.2:

$$\tau_{\max} = \frac{3 \times F_{\max}}{4 \times w \times t} \quad (2)$$

where F_{\max} is the maximum force in N, w is the specimen width (mm) and t is the specimen thickness (mm).

Dynamic Mechanical Analysis (DMA). Mechanical testing by DMA assesses the mechanical response of the laminates according to the temperature. The tests consist of a three-point bending in the transverse-to-fibre direction. For each manufacturing conditions investigated, two samples were tested on a Mettler TOLEDO DMA 1. The scans were performed from room temperature to 250°C at a scanning speed of 2 °C/min. A frequency of 1 Hz and a displacement amplitude of 3 µm were used. The peak value of the loss factor $\tan \delta$ was obtained by a mathematical treatment in Matlab, which consisted of fitting the baseline and smoothing the curve to extract the maximum value of $\tan \delta$.

Results and discussion

Overall laminate quality. The results of the mean signal amplitude measured by ultrasonic nondestructive control of plates are shown in Table 2. Through C-Scan measurement, a global material health difference between 25/350 and 250/350 is observed with an increase of the transmitted US signal amplitude from 30 to 35 %SH respectively. An equivalent increase in amplitude of 5%SH between 25/450 and 250/450 is also observed, showing a better material quality of the plates produced on a heated tool. However, the effect of the TT is small compared to the effect of the LST, as there is approximately a 45 %SH rise in amplitude with an increase of LST from 350 to 450 °C.

Microscopy observations of manufactured panels are presented in Fig. 2. Void contents were measured for all laminates, and the interply and intraply void contents are listed in Table 2. Such information allow to discriminate porosities resulting from the lack of intimate contact and those generated by deconsolidation phenomena. The former is visible by a high interply void content, while the latter can be associated with a higher intraply void content as compared to the initial tape [6], [14]. At first glance, the evolution of void content with the changing of the LST and the TT follows the same trend as the evolution of the US signal amplitude discussed previously. However, when considering the location of voids, three different cases can be highlighted: the 25/350 contains both interply and intraply voids, the 250/350 rather contains intraply voids and almost no interply voids, and the 25/450 and 250/350 show only a small amount of intraply voids, slightly higher than the initial void content of the tape. Through these observations, we can conclude that only the laminate 25/350 presents a lack of intimate contact at the welded interface, indicating that its establishment is promoted by increasing the TT or the LST.

Indeed, the observations of Celik et al. [17] on a PEEK/CF demonstrated the establishment of the intimate contact at a TT of 155 °C (and a LST of 380-400 °C), as compared to similar lay-up on an unheated tool. However, it is important to remember that in this latter study and all others referenced in this article, comparison with literature data is limited by differences in material composition. The favourable conditions for the establishment of intimate contact and healing when the tool is heated over the T_g can be explained by an increased time above T_g and by a lower cooling rate [1], [18], [19]. Hence, for the 25/350 condition, even if the T_m is reached, there might not be enough time left to activate these consolidation mechanisms.

If we one focus now on intraply void related to deconsolidation, one could notice that laminates welded at 350 °C are much more concerned by this phenomenon. A proposed assumption to

explain deconsolidation by increasing intraply void content is sufficient time for void growth and frozen-in-fibre stress release during the heating phase prior to consolidation under the roller, combined with a too short time under pressure for allowing the squeeze flow mechanisms to fill the voids with matrix. Hence, the difference between the 250/350 and the laminates welded at 450 °C could be explained by the material viscosity which affect the establishment of the consolidation by squeeze flow: the matrix of the laminate 250/350 could have a sufficiently low viscosity to deconsolidate, but a too high viscosity to fill in all the voids during the application of pressure. This assumption is based on an almost 10-fold difference in viscosity of PEEK between 350 °C and 450 °C [20].

Finally, the intraply void content of laminates welded at 450 °C is slightly higher than the void content of the as-received tape, reflecting a little deconsolidation for these manufacturing conditions. The void content of an autoclaved manufactured laminate from literature ([15]₀ CF/PEEK consolidated in autoclave at 370 °C during 20 min under a pressure of 7 bar, and cooled at 2 °C/min) is presented in Table 2 and in Fig. 4[15]. While a void content respecting the standard criterion for most aerospace applications (lower than 1 % [1]) is reached for a LST at 450 °C with our material system and processing conditions, we notice that it is possible to reach lower void content by autoclave, when maximum consolidation is achieved.

Table 2 – Void content results

	25/350	250/350	25/450	250/450	autoclaved-manufactured reference [15]	as-received tape
US amplitude [%SH]	30	35	75	80	-	-
Interply void content [%]	3.12 ± 0.7	0,11 ± 0.02	0.06 ± 0.02	0.02 ± 0.01	0.08	-
Intraply void content [%]	2.35 ± 0.3	2.71 ± 0.2	0.75 ± 0.2	0.69 ± 0.2		0.49 ± 0.4

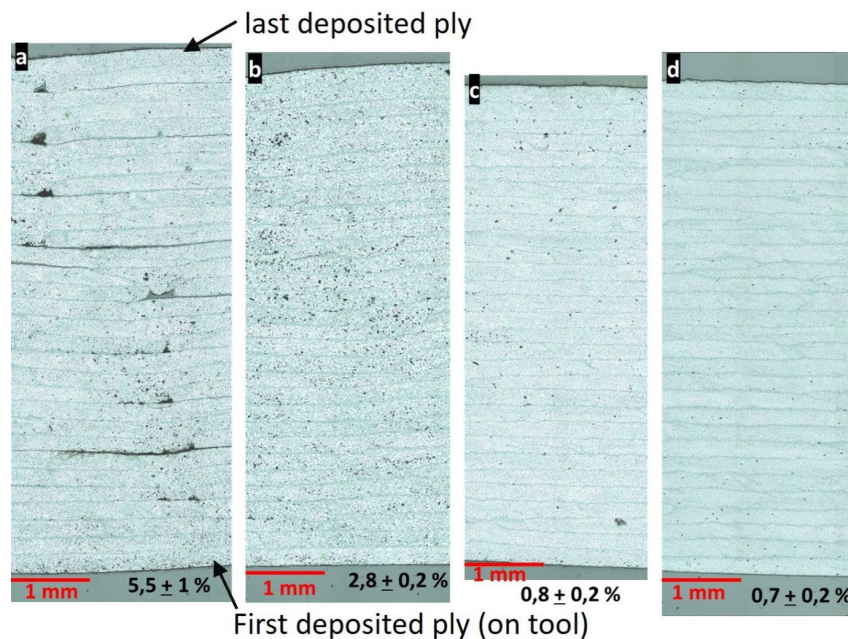


Figure 2 – Images of cross-section laminates (a) 25/350, (b) 250/350, (c) 25/450 and (d) 250/450 with the associated void content

ILSS mechanical performances. On the load-displacement curves presented in Fig. 3a., we can clearly see a different mechanical behavior in sample 25/350, which drops significantly at a low load, compared to the other specimens presenting nonlinear response and higher values for load and displacement at failure. The combined observations of cross-section of fracture (Fig. 3b and c.) and fracture surfaces on SEM (Fig. 3d and e) confirm a different behavior of 25/350 specimens. This laminate, which have a high interply void content, failed at a welded interface due to an interlaminar shear mechanism. Fracture surfaces of the specimens are comprised of a smooth resin layer with few bare fibres. For the three other laminates, having mainly intraply voids, the maximum load varies (Fig. 3a) but they all break by an intralaminar shear mode, and especially at the fibre-matrix interfaces, as shown in Fig. 3e. on the 250/350 condition. This result means that when processing parameters are favorable for intimate contact and healing establishment (even if healing is not complete), the welded interface is no longer the weakest area of the laminate when subjected to out-of-plane shear loading. It explains why the ILSS values of these laminates are close among each other compared to the ILSS value of the 25/350 laminates (Fig. 3a).

Furthermore, the difference of behavior between all the specimens correlates with the void content, which decreases when the apparent ILSS strength increases (Fig.4a). A correlation is found between the intraply void content and the ILSS values when the failure mode is intralaminar. It would be interesting to know the failure mode of the autoclave laminate from literature [15] (previously presented) to confirm the relation established in the well-consolidated laminates of this study. However, even if these results highlight an obvious effect of intraply void content on ILSS, the understanding of fracture mechanisms during ILSS testing is necessary to confirm that state. Also, Gao & Kim [21] showed that fast cooling of semi-crystalline thermoplastic reduces the thickness of the transcrystalline region around the fibres, leading to a weaker fibre-matrix interface. Hence, for low intraply void contents (at a LST of 450 °C), the increase in ILSS by increasing the TT at 250 °C may be in agreement with this latter statement, because these conditions may promote the crystallization of PEEK [18]. To explain the different ILSS values between 25/450 and 250/450 presenting no significant differences in intraply void content, the characterization of the crystallinity of PEEK is then required.

Also, Fig. 4a shows that the ILSS value of the PEEK/CF autoclave reference is significantly higher than the ILSS values of the LAMP laminate obtained in this study. However, the authors specified that this high ILSS value of autoclave reference is due to a high crystallinity (40%).

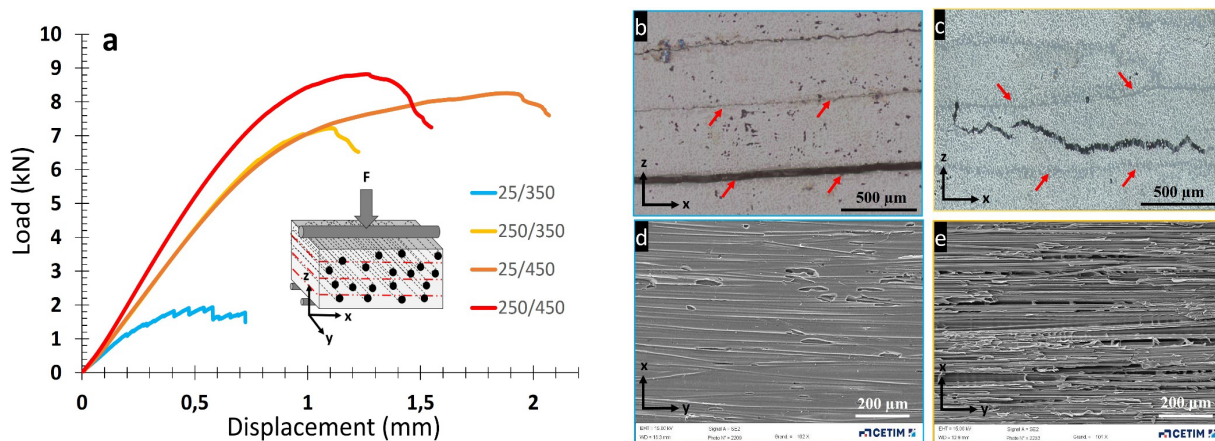


Figure 3 – a) Load curves for the different manufacturing conditions; post-mortem cross-section images of ILSS laminates (b) 25/350 and (c) 250/350 where red arrows indicate the inter-ply position; fracture surfaces (by SEM) of ILSS laminates (d) 25/350 and (e) 250/350

Crystallinity. Results of degree of crystallinity obtained by DSC analysis are presented in Fig. 4b and they show a higher effect of the LST on the degree of crystallinity than the TT. However, due to the size of sampling in DSC and the sensitivity limiting detection of low variation of heat flux (especially for the cold crystallization) and measured enthalpies to experimental repetitiveness and presence of carbon fibers, we obtained more accurate (through indirect) and repetitive information by DMA analysis to assess an evolution of the crystallinity with the manufacturing conditions.

DMA. A correlation between the viscoelastic behavior of the laminates and their degree of crystallinity was performed by DMA analysis. The goal was to assess the variation of the $\tan \delta$ loss factor peak and its corresponding temperature (Fig. 4b), which is considered as the glass transition temperature T_g , with LST and TT. Only the variation of $\tan \delta$ will be discussed in this paper. This value is defined by the ratio between the loss and the storage modulus, explaining the reverse link between $\tan \delta$ and the degree of crystallinity because increasing the crystallinity is equivalent to decreasing the amorphous chain mobility, even if this latter also depends on the morphology (type and size of the crystals).

By comparing LSTP and autoclave PEEK/CF laminates, Ray et al. [22] showed an increase of T_g from 140 °C to 153 °C and a decrease in $\tan \delta$ from 0,075 to 0,03 related to an increase in crystallinity from 17,6% to 42%. Also, the effect of TT on the T_g has been already observed in a PEEK/CF laminate manufactured by SPIDE TP® by El Bayssari [23] : a variation of T_g from 140 °C to 148 °C when the tool is heated at 180 °C was noted.

As shown in Fig. 4b, our results confirmed this trend. There is a significant drop of $\tan \delta$ when increasing the TT. This drop takes place from values of $\tan \delta$ of 0,18 to 0,10 in the laminates manufactured with a LST of 350 °C and from 0,15 to 0,1 in the laminates manufactured at 450°C. However, there is probably an effect of the void content on the T_g and $\tan \delta$ values measured by DMA [24]. In order to decorrelate these effects, one can comparatively evaluate the $\tan \delta$ and T_g from cooling curves, assuming all cold crystallization was completed during the temperature ramp until 250°C (crystallization occurs in a few seconds at this temperature according to Tardif et al. [25]) and that this ramp do not affect the porosity content. In this way, it can be assumed that all specimens are all fully crystallized during the cooling down phase, and that differences in T_g and $\tan \delta$ between the laminates can only be attributed to differences in porosity contents. Hence, the differences between laminates observed during the ramp-up can then be analyzed to evaluate qualitatively the influence of crystallinity variations between laminates. This evaluation is not presented here as it is still in progress, however the comparison of $\tan \delta$ and T_g remains valid for the 25/450 and 250/450, for which the void contents are similar. Considering these laminates, it is clearly seen that the drop in $\tan \delta$ could be related to a rise in the crystallinity of the material. This observation could reveal that for laminates containing similar void content, any small variation of the degree of crystallinity may has an influence on the intralaminar resistance. Particularly, a drop of 33 % of the $\tan \delta$ value is responsible of a rise of 6 % of the ILSS value (i.e Fig. 4a and b). An effect of the crystallinity of the material on its ILSS value has already been emphasized by the observations of Gao and Kim [26]. They showed variation in ILSS values from approximately 80 to 55 MPa when the degree of crystallinity varied from approximately 38 to 13 %. However, no investigation was performed about void content and laminates were manufactured by hot press in this study.

Finally, the higher degree of crystallinity for laminates manufactured on a heated tool at 250 °C or at a Laser Setpoint temperature of 450 °C is in accordance with thermal modelling predicting longer time above T_g under these conditions, and consequently a longer time to crystallize [18], [19].

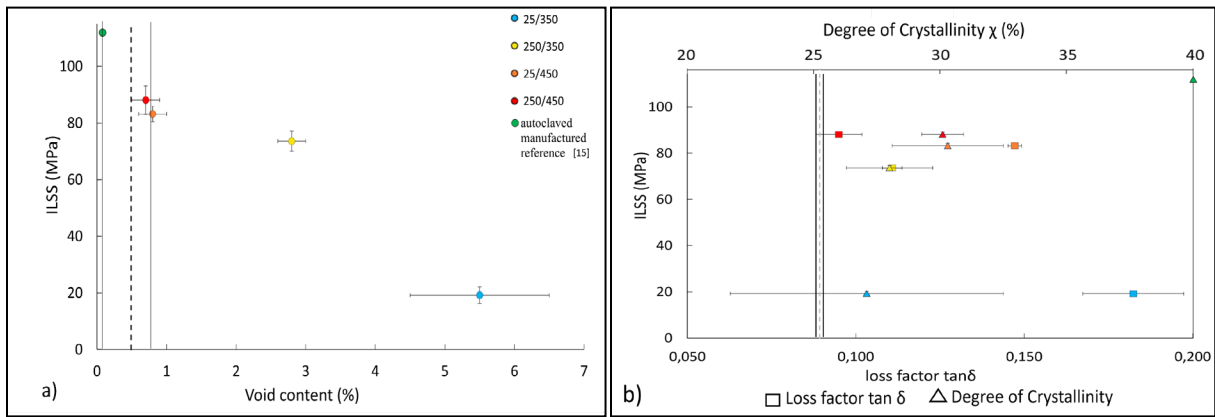


Figure 4 – For all manufacturing conditions investigated: a) ILSS data according to the void content, with black dashed lines representing the as-received tape void content b) ILSS data according to the degree of crystallinity measured by DSC and the loss factor $\tan \delta$ assessed by DMA. Grey dashed lines corresponding to the as-received tape degree of crystallinity

Conclusion

In this work, the characterization of PEEK/CF laminates processed using several LAMP manufacturing conditions was performed.

To observe the effect of the process temperature and the cooling rate inside the material, the two processing parameters that were varied are the laser setpoint temperature (LST) (350 and 450 °C), and the tool temperature (TT) (25 and 250 °C). Then the laminates void content and distribution, crystallinity, viscoelastic and shear behaviors were investigated.

Firstly, it was shown that the LST and the TT affect the overall laminate qualities. The ultrasonic signal amplitude was much high for laminates manufactured at 450 °C compared to laminates manufactured at 350°C. This trend was confirmed by microscopy observations of the cross-section of the laminates showing a higher void content for the latter.

In order to determine the voids repartition, the measurement of interply and intraply void content was carried out. Results highlighted the lack of intimate contact for the laminate processed at 350 °C on an unheated tool, resulting in interply void content of 4%. Although the laminate welded at 350 °C on a tool heated at 250 °C has a lower interply void content (0,8 %), it contains much more intraply voids (3 %) than the laminates manufactured at 450 °C (about 0,7 %), whatever the TT. It has been speculated that the deconsolidation by increasing the intraply void content is due to a growth of initial void content and the development of cavities around fiber due to relaxation of stress at the fiber-matrix interfaces during the heating phase.

Secondly, a correlation between void distribution, ILSS results and failure mode was demonstrated. For laminates processed at 350 °C on an unheated tool, showing a lack of intimate contact, the interlaminar failure mode is obviously governed by the presence of interply voids. Unsurprisingly, this laminate has the lowest ILSS value.

Finally, the characterization of the degree of crystallinity by DSC and DMA allowed to link this property to the ILSS of the laminates. For well-consolidated laminate having mainly intralaminar voids, both the intraply void content and the crystallinity of the laminate seem to be related to the apparent ILSS performances and further investigation are in progress in order to clearly decorrelate both effects.

References

- [1] R. Arquier, I. Iliopoulos, G. Régner, and G. Miquelard-Garnier, “Consolidation of continuous-carbon-fiber-reinforced PAEK composites: a review,” *Mater Today Commun*, vol. 32, p. 104036, 2022. <https://doi.org/10.1016/j.mtcomm.2022.104036>

- [2] W. Il Lee and G. S. Springer, “A Model of the Manufacturing Process of Thermoplastic Matrix Composites,” *J Compos Mater*, vol. 21, no. 11, pp. 1017–1055, 1987. <https://doi.org/10.1177/002199838702101103>
- [3] F. Yang and R. Pitchumani, “Healing of thermoplastic polymers at an interface under nonisothermal conditions,” *Macromolecules*, vol. 35, no. 8, pp. 3213–3224, Apr. 2002. <https://doi.org/10.1021/ma010858o>
- [4] F. Dave, M. M. Ali, R. Sherlock, A. Kandasami, and D. Tormey, “Laser transmission welding of semi-crystalline polymers and their composites: A critical review,” *Polymers*, vol. 13, no. 5. MDPI AG, pp. 1–52, Mar. 01, 2021. <https://doi.org/10.3390/polym13050675>
- [5] A. Yousefpour, M. Hojjati, and J. P. Immarigeon, “Fusion bonding/welding of thermoplastic composites,” *Journal of Thermoplastic Composite Materials*, vol. 17, no. 4. pp. 303–341, Jul. 2004. <https://doi.org/10.1177/0892705704045187>
- [6] T. K. Slange, L. L. Warnet, W. J. B. Grouve, and R. Akkerman, “Deconsolidation of C/PEEK blanks: on the role of prepreg, blank manufacturing method and conditioning,” *Compos Part A Appl Sci Manuf*, vol. 113, pp. 189–199, Oct. 2018. <https://doi.org/10.1016/j.compositesa.2018.06.034>
- [7] O. Çelik, A. Choudhary, D. Peeters, J. Teuwen, and C. Dransfeld, “Deconsolidation of thermoplastic prepreg tapes during rapid laser heating,” *Compos Part A Appl Sci Manuf*, vol. 149, Oct. 2021. <https://doi.org/10.1016/j.compositesa.2021.106575>
- [8] L. Amedewovo, L. Orgéas, B. de Parscau du Plessix, N. Lefevre, A. Levy, and S. Le Corre, “Deconsolidation of carbon fiber-reinforced PEKK laminates: 3D real-time in situ observation with synchrotron X-ray microtomography,” *Compos Part A Appl Sci Manuf*, vol. 177, Feb. 2024. <https://doi.org/10.1016/j.compositesa.2023.107917>
- [9] K. Yassin and M. Hojjati, “Processing of thermoplastic matrix composites through automated fiber placement and tape laying methods: A review,” *Journal of Thermoplastic Composite Materials*, vol. 31, no. 12. SAGE Publications Ltd, pp. 1676–1725, Dec. 01, 2018. <https://doi.org/10.1177/0892705717738305>
- [10] R. Arquier, H. Sabatier, I. Iliopoulos, G. Régnier, and G. Miquelard-Garnier, “Role of the inter-ply microstructure in the consolidation quality of high-performance thermoplastic composites,” *Polym Compos*, 2023. <https://doi.org/10.1002/pc.27847>
- [11] M. Bonmatin, F. Chabert, G. Bernhart, T. Cutard, and T. Djilali, “Ultrasonic welding of CF/PEEK composites: Influence of welding parameters on interfacial temperature profiles and mechanical properties,” *Compos Part A Appl Sci Manuf*, vol. 162, Nov. 2022. <https://doi.org/10.1016/j.compositesa.2022.107074>
- [12] C. Zhang *et al.*, “Effect of porosity and crystallinity on mechanical properties of laser in-situ consolidation thermoplastic composites,” *Polymer (Guildf)*, vol. 242, Mar. 2022. <https://doi.org/10.1016/j.polymer.2022.124573>
- [13] J. Chen, K. Fu, and Y. Li, “Understanding processing parameter effects for carbon fibre reinforced thermoplastic composites manufactured by laser-assisted automated fibre placement (AFP),” *Compos Part A Appl Sci Manuf*, vol. 140, Jan. 2021. <https://doi.org/10.1016/j.compositesa.2020.106160>
- [14] Z. Qureshi, T. Swait, R. Scaife, and H. M. El-Dessouky, “In situ consolidation of thermoplastic prepreg tape using automated tape placement technology: Potential and

possibilities,” *Compos B Eng*, vol. 66, pp. 255–267, 2014. <https://doi.org/10.1016/j.compositesb.2014.05.025>

[15] A. J. Comer *et al.*, “Mechanical characterisation of carbon fibre-PEEK manufactured by laser-assisted automated-tape-placement and autoclave,” *Compos Part A Appl Sci Manuf*, vol. 69, pp. 10–20, Feb. 2015. <https://doi.org/10.1016/j.compositesa.2014.10.003>

[16] D. J. Blundell and B. N. Osborn, “The morphology of poly(aryl-ether-ether-ketone).”

[17] O. Çelik, D. Peeters, C. Dransfeld, and J. Teuwen, “Intimate contact development during laser assisted fiber placement: Microstructure and effect of process parameters,” *Compos Part A Appl Sci Manuf*, vol. 134, Jul. 2020. <https://doi.org/10.1016/j.compositesa.2020.105888>

[18] F. O. Sonmez and H. T. Hahn, “Analysis of the on-line consolidation process in thermoplastic composite tape placement,” *Journal of Thermoplastic Composite Materials*, vol. 10, no. 6, pp. 543–572, 1997. <https://doi.org/10.1177/089270579701000604>

[19] C. M. Stokes-Griffin and P. Compston, “Investigation of sub-melt temperature bonding of carbon-fibre/PEEK in an automated laser tape placement process,” *Compos Part A Appl Sci Manuf*, vol. 84, pp. 17–25, May 2016. <https://doi.org/10.1016/j.compositesa.2015.12.019>

[20] M. A. Khan, P. Mitschang, and R. Schledjewski, “Identification of some optimal parameters to achieve higher laminate quality through tape placement process,” in *Advances in Polymer Technology*, Jun. 2010, pp. 98–111. <https://doi.org/10.1002/adv.20177>

[21] S. L. Gao and J. K. Kim, “Correlation among crystalline morphology of PEEK, interface bond strength, and in-plane mechanical properties of carbon/PEEK composites,” *J Appl Polym Sci*, vol. 84, no. 6, pp. 1155–1167, Feb. 2002. <https://doi.org/10.1002/app.10406>

[22] D. Ray *et al.*, “Fracture toughness of carbon fiber/polyether ether ketone composites manufactured by autoclave and laser-assisted automated tape placement,” *J Appl Polym Sci*, vol. 132, no. 11, Mar. 2015. <https://doi.org/10.1002/app.41643>

[23] A. Maria El Bayssari, “Study and comprehension of the residual stresses and strains state in thermoplastic composite materials manufactured by tape placement.” [Online]. Available: <https://theses.hal.science/tel-03888045>

[24] P. A. Rodriguez and D. W. Radford, “A DMA-Based Approach to Quality Evaluation of Digitally Manufactured Continuous Fiber-Reinforced Composites from Thermoplastic Commingled Tow,” *Journal of Composites Science*, vol. 6, no. 2, Feb. 2022. <https://doi.org/10.3390/jcs6020061>

[25] X. Tardif *et al.*, “Experimental study of crystallization of PolyEtherEtherKetone (PEEK) over a large temperature range using a nano-calorimeter,” *Polym Test*, vol. 36, pp. 10–19, 2014. <https://doi.org/10.1016/j.polymertesting.2014.03.013>

[26] S. L. Gao and J. K. Kim, “Correlation among crystalline morphology of PEEK, interface bond strength, and in-plane mechanical properties of carbon/PEEK composites,” *J Appl Polym Sci*, vol. 84, no. 6, pp. 1155–1167, Feb. 2002. <https://doi.org/10.1002/app.10406>